

# Thorium-doping induced superconductivity up to 56 K in $\text{Gd}_{1-x}\text{Th}_x\text{FeAsO}$

Cao Wang, Linjun Li, Shun Chi, Zengwei Zhu, Zhi Ren, Yuke Li, Yuetao Wang, Xiaolin, Yongkang Luo, Shuai Jiang, Xiangfan Xu, Guanghan Cao\* and Zhu'an Xu†  
*Department of Physics, Zhejiang University, Hangzhou 310027, People's Republic of China*

Following the discovery of superconductivity in an iron-based arsenide  $\text{LaO}_{1-x}\text{F}_x\text{FeAs}$  with a superconducting transition temperature ( $T_c$ ) of 26 K[1],  $T_c$  was pushed up surprisingly to above 40 K by either applying pressure[2] or replacing La with Sm[3], Ce[4], Nd[5] and Pr[6]. The maximum  $T_c$  has climbed to 55 K, observed in  $\text{SmO}_{1-x}\text{F}_x\text{FeAs}$ [7, 8] and  $\text{SmFeAsO}_{1-x}$ [9]. The value of  $T_c$  was found to increase with decreasing lattice parameters in  $\text{LnFeAsO}_{1-x}\text{F}_x$  (Ln stands for the lanthanide elements) at an apparently optimal doping level. However, the  $\text{F}^-$  doping in  $\text{GdFeAsO}$  is particularly difficult[10, 11] due to the lattice mismatch between the  $\text{Gd}_2\text{O}_2$  layers and  $\text{Fe}_2\text{As}_2$  layers. Here we report observation of superconductivity with  $T_c$  as high as 56 K by the  $\text{Th}^{4+}$  substitution for  $\text{Gd}^{3+}$  in  $\text{GdFeAsO}$ . The incorporation of relatively large  $\text{Th}^{4+}$  ions relaxes the lattice mismatch, hence induces the high temperature superconductivity.

$\text{LnFeAsO}$  family[12] crystalline in tetragonal  $\text{ZrCuSiAs}$ -type[13] structure with space group  $P4/nmm$ . From the crystal chemistry point of view, the crystal structure can be described as an alternate stacking of  $\text{Ln}_2\text{O}_2$  fluorite-type block layers and  $\text{Fe}_2\text{As}_2$  antiferrotype block layers along  $c$ -axis. The two block layers are connected by  $\text{CsCl}$ -type layers (Figure 1). Therefore, the chemical stability of  $\text{LnFeAsO}$  depends, to some extent, on the lattice match between the two block layers. A rough estimate based on the effective ionic radii[14] indicates that the  $\text{Ln}_2\text{O}_2$  planar lattice is substantially smaller than the  $\text{Fe}_2\text{As}_2$  lattice. The lattice mismatch becomes more serious for the  $\text{LnFeAsO}$  member with a smaller  $\text{Ln}^{3+}$  ion. That may explain why  $\text{TbFeAsO}$ ,  $\text{DyFeAsO}$  and other heavy-lanthanide-containing  $\text{LnFeAsO}$  members were hard to synthesize previously[12].

As the family member with the relatively small  $\text{Ln}^{3+}$  ion,  $\text{GdFeAsO}$  is a promising parent compound to have a higher  $T_c$  through carrier doping. Similar to cuprate superconductors in which superconductivity emerges when charge carriers are induced into  $\text{CuO}_2$  planes by chemical doping at "charge reservoir layers", [15] superconductivity in  $\text{LnFeAsO}_{1-x}\text{F}_x$  is realized by partial substitution of  $\text{O}^{2-}$  with  $\text{F}^-$ . The  $\text{F}^-$ -for- $\text{O}^{2-}$  substitution introduces extra positive charges in the insulat-

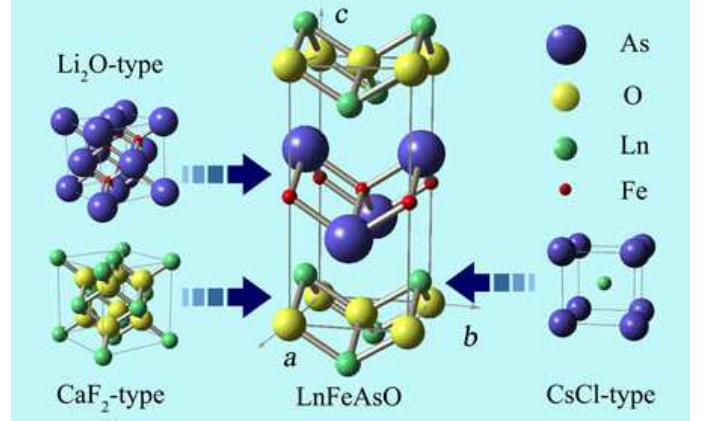


FIG. 1: Crystal chemistry understanding of the structure of  $\text{LnFeAsO}$  (Ln=lanthanides). The stacking of fluorite ( $\text{CaF}_2$ ) layers,  $\text{CsCl}$ -type layers and antiferrotype ( $\text{Li}_2\text{O}$ ) layers along  $c$ -axis forms the  $\text{LnFeAsO}$  structure. The lattice constant along the stacking direction can be expressed by the formula  $c \simeq \frac{1}{2}a_{\text{CaF}_2} + \frac{1}{2}a_{\text{CsCl}} + \frac{1}{2}a_{\text{Li}_2\text{O}}$ , which basically satisfies the experimental result. Note that the lattice mismatch between the  $\text{Ln}_2\text{O}_2$  layers and the  $\text{Fe}_2\text{As}_2$  layers affects the chemical stability of  $\text{LnFeAsO}$ .

ing  $\text{Ln}_2\text{O}_2$  layers and negative charges (electron doping) in the  $\text{Fe}_2\text{As}_2$  layers. Earlier preliminary experiment showed sign of superconductivity below 10 K in  $\text{GdFeAsO}_{1-x}\text{F}_x$ . [10] Later,  $T_c$  was pushed up to 36 K in a polycrystalline sample with a nominal composition of  $\text{GdO}_{0.83}\text{F}_{0.17}\text{FeAs}$ . [11] Very recently the  $T_c$  value was increased to 53.5 K in oxygen-deficient  $\text{GdFeAsO}_{1-x}$  by using high-pressure synthesis. [16] It is of great interest whether the  $T_c$  can be elevated further in electron-doped  $\text{GdFeAsO}$  systems.

Up to now, electron doping in the iron-based arsenides was realized through the chemical substitution only at oxygen site in  $\text{Ln}_2\text{O}_2$  layers. Because the ionic radius of  $\text{F}^-$  (1.31 Å, CN=4) is distinctly smaller than that of  $\text{O}^{2-}$  (1.38 Å, CN=4) [14],  $\text{F}^-$  substitution for  $\text{O}^{2-}$  in  $\text{GdFeAsO}$  leads to more severe lattice mismatch as mentioned above. In other word, doping  $\text{F}^-$  (or oxygen vacancy) in  $\text{GdFeAsO}$  is particularly difficult, which is probably the main obstacle to elevate  $T_c$ . Substitution of  $\text{Ln}^{3+}$  by relatively large tetravalence ions is an alternative route to introduce electrons. A successful example was the electron doping in  $\text{Ln}_{2-x}\text{Ce}_x\text{CuO}_4$  (Ln=Pr, Nd or Sm), which has led to the discovery of  $n$ -type cuprate superconductors [17].  $\text{Th}^{4+}$  is a very stable tetravalence ions and is as large as  $\text{Gd}^{3+}$  [14], therefore, we pursued the  $\text{Th}^{4+}$  substitution for  $\text{Gd}^{3+}$  in the  $\text{GdFeAsO}$  system.

\*Electronic address: ghcao@zju.edu.cn

†Electronic address: zhuan@zju.edu.cn

Figure 2a shows the X-ray diffraction (XRD) patterns of the  $\text{Gd}_{1-x}\text{Th}_x\text{FeAsO}$  samples. The XRD peaks of the undoped compound can be well indexed based on the tetragonal  $\text{ZrCuSiAs}$ -type structure, indicating single phase of  $\text{GdFeAsO}$ . As for the Th-doped samples, small amount of unreacted  $\text{ThO}_2$  can be seen. The refined lattice parameters are  $a = 3.9154(2)$  Å and  $c = 8.4472(4)$  Å for the parent compound, basically consistent with the previously reported values[12]. For the Th-doped sample of  $x=0.2$ , the fitted lattice parameters are  $a = 3.9161(2)$  Å and  $c = 8.4386(3)$  Å. The other Th-doped sample of  $x=0.25$  has a similar unit cell with  $a=3.9166(3)$  Å and  $c = 8.4382(5)$  Å. Therefore, it is evident that the Th-doping tends to expand the lattice within  $ab$ -planes but to shorten the lattice along the  $c$ -axis. The substantial change in cell constants indicates that thorium is incorporated in the lattice. Meanwhile, the  $ab$ -plane expansion reflects the effective electron doping onto FeAs layers.

More direct evidence of Th incorporation into the lattice comes from the chemical composition measurement by energy-dispersive X-ray (EDX) microanalysis. Figure 2b shows that the microcrystal in the SEM image contains remarkably Th in addition to Gd, O, Fe and As. Quantitative analysis gives the Gd:Th:Fe:As ratios as 0.83:0.19:0.96:1.00 for the  $x=0.2$  sample (Here we omit the oxygen content because the amount of oxygen cannot be measured so precisely by EDX technique). This result demonstrates that most of the Th was successfully doped for the sample of  $x=0.2$ . Obviously, Th-doping level is higher than that of F-doping in  $\text{GdFeAsO}$ [10, 11].

Figure 3a shows the  $\rho(T)$  curve for  $\text{Gd}_{1-x}\text{Th}_x\text{FeAsO}$  samples. For the undoped  $\text{GdFeAsO}$ , the  $\rho(T)$  curve exhibits an obvious anomaly at 128 K, characterized by a resistivity drop with decreasing temperature. In  $\text{LaFeAsO}$  a similar resistivity anomaly was found at 150 K,[1, 18] which has been recently suggested to be associated with a structural phase transition and/or an antiferromagnetic spin-density-wave transition[18, 19, 20, 21]. We speculate that the present resistivity anomaly in  $\text{GdFeAsO}$  has a similar physical origin with that in  $\text{LaFeAsO}$ . For  $x=0.2$  and  $x=0.25$ , such resistivity anomaly disappears, instead, resistivity drops abruptly to zero below 55 K, indicating a superconducting transition. In addition, the linear temperature-dependence of normal-state resistivity near  $T_c$  suggests possible non-Fermi liquid behavior in the present system, similar to that in  $\text{SmFeAsO}_{1-x}\text{F}_x$ [8].

The magnetic measurement on  $\text{Gd}_{1-x}\text{Th}_x\text{FeAsO}$  samples was shown in Figure 3b. In the parent compound, the high-temperature magnetic susceptibility ( $\chi$ ) follows the Curie-Weiss law. The fitted effective magnetic moments was  $7.96 \mu_B$  per formula unit, in good agreement with the magnetic moment of free  $\text{Gd}^{3+}$  ion. Below 4.2 K,  $\chi$  drops sharply, indicating an antiferromagnetic ordering of  $\text{Gd}^{3+}$  magnetic moments. Note that similar behavior was observed in  $\text{SmFeAsO}$  where the Neel temperature was 4.6 K.[22]

For the Th-doped samples, e.g.,  $x=0.2$ , the normal-

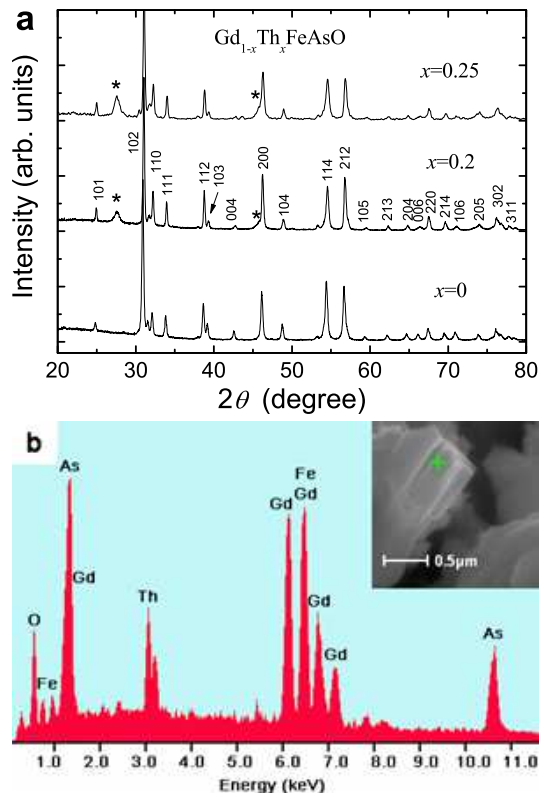


FIG. 2: **Phase and compositional analysis of  $\text{Gd}_{1-x}\text{Th}_x\text{FeAsO}$  samples.** **a**, Powder XRD of  $\text{Gd}_{1-x}\text{Th}_x\text{FeAsO}$  polycrystalline samples. The asterisked peaks come from unreacted  $\text{ThO}_2$ . **b**, a representative EDX spectrum of a crystalline grain of  $\text{Gd}_{0.8}\text{Th}_{0.2}\text{FeAsO}$  sample, indicating the incorporation of thorium into the lattice. The inset shows the SEM image of the identical sample. The marked spot is the position where the EDX spectrum was collected.

state susceptibility roughly obeys Curie-Weiss law. Below 55 K,  $\chi$  drops steeply to negative values, confirming the superconductivity observed above. After subtracting the paramagnetic susceptibility of  $\text{Gd}^{3+}$  ions, the volume fraction of magnetic shielding at 10 K was estimated to be over 50%, indicating bulk superconductivity. The differential  $\chi_{FC}$  curve in the inset of Figure 3b shows that the  $T_c(\text{onset})$  is over 56 K, consistent with the resistance measurement. Therefore, Th-doping in  $\text{GdFeAsO}$  elevates the  $T_c$  by 20 K ( $T_c=36$  K in  $\text{GdO}_{0.83}\text{F}_{0.17}\text{FeAs}$ [11]). Moreover, the  $T_c$  of 56 K is among the highest ever discovered in iron-based oxypnictides.

Our observation of superconductivity in  $\text{Gd}_{1-x}\text{Th}_x\text{FeAsO}$  indicates that the Ln-site substitution in  $\text{LnFeOAs}$  is feasible to realize electron doping, hence the high temperature superconductivity. Moreover, the electron-doping is more easily induced by the  $\text{Th}^{4+}$ -substitution compared with the  $\text{F}^-$ -substitution in  $\text{GdFeOAs}$ . This manifests that the lattice match between  $\text{Ln}_2\text{O}_2$  fluorite-type layers and  $\text{Fe}_2\text{As}_2$  antiferrotype layers is important not only for the chemical stability of

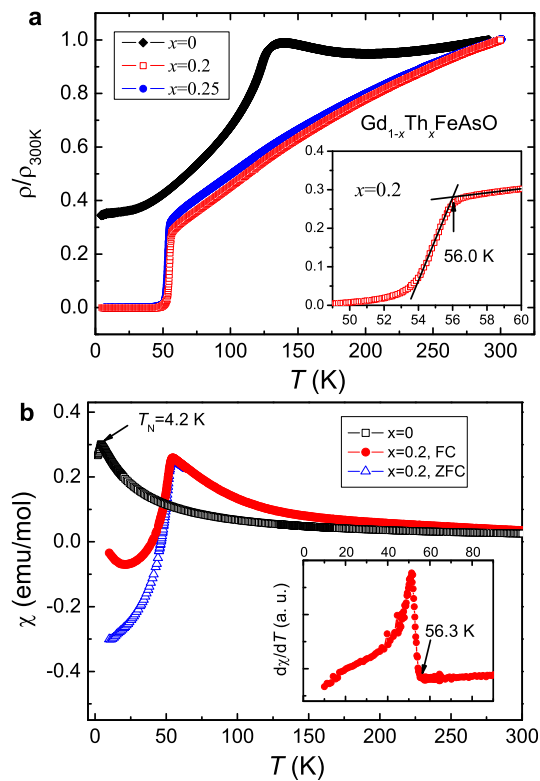


FIG. 3: **Electrical resistivity ( $\rho$ ) and magnetic susceptibility ( $\chi$ ) of  $\text{Gd}_{1-x}\text{Th}_x\text{FeAsO}$ .** **a**,  $\rho$  versus  $T$ . The data are normalized to  $\rho_{300\text{K}}$  as the resistivity measured on polycrystalline samples is often higher than the intrinsic value due to the grain boundary and surface effect. The inset is an expanded plot to show the superconducting transition at 56 K for the sample of  $x=0.2$ . **b**,  $\chi$  versus  $T$ . The lower inset shows the differential  $\chi_{FC}$  curve of  $\text{Gd}_{0.8}\text{Th}_{0.2}\text{FeAsO}$  powder sample, which locates the onset  $T_c$  at 56.3 K. ZFC, zero-field cooling; FC, field cooling.

the parent compounds, but also for the electron-doping level in  $\text{LnFeAsO}$ . It is thus expected that the thorium-doping strategy can be applied to other iron-based oxypnictides.

## METHODS

### Sample preparation

Polycrystalline samples of  $\text{Gd}_{1-x}\text{Th}_x\text{FeAsO}$  were synthesized by solid state reaction in an evacuated quartz

tube. All the starting materials ( $\text{Gd}$ ,  $\text{Gd}_2\text{O}_3$ ,  $\text{ThO}_2$ ,  $\text{Fe}$  and  $\text{As}$ ) are with high purity ( $\geq 99.95\%$ ). First,  $\text{GdAs}$  was presynthesized by reacting  $\text{Gd}$  tapes with  $\text{As}$  pieces in vacuum at 773 K for 10 hours and then 1173 K for 12 hours. Similarly,  $\text{FeAs}$  was prepared by reacting  $\text{Fe}$  powders with  $\text{As}$  shots at 773 K for 6 hours and then 1030 K for 12 hours. Then, powders of  $\text{GdAs}$ ,  $\text{Gd}_2\text{O}_3$ ,  $\text{ThO}_2$ ,  $\text{Fe}$  and  $\text{FeAs}$  were weighed according to the stoichiometric ratio of  $\text{Gd}_{1-x}\text{Th}_x\text{FeAsO}$ . The weighed powders were mixed thoroughly by grinding, and pressed into pellets under a pressure of  $4000 \text{ kg/cm}^2$  in an argon-filled glove box. The pressed pellets were wrapped with Ta foils, and sealed in an evacuated quartz ampoule. The sealed ampoule was slowly heated to 1423 K, holding for 48 hours. Finally the samples were rapidly cooled to room temperature.

### Structural characterizations

Powder X-ray diffraction was performed at room temperature using a D/Max-rA diffractometer with  $\text{Cu K}\alpha$  radiation and a graphite monochromator. The XRD diffractometer system was calibrated using standard Si powders. Lattice parameters were refined by a least-squares fit using at least 20 XRD peaks. Energy-dispersive X-ray (EDX) spectra were obtained by using the Phoenix EDAX equipment attached to a field-emission scanning electron microscope (SIRION FEI). The ground sample powders were placed directly on the copper sample holder for making the SEM specimen.

### Electrical and magnetic measurements

The electrical resistivity was measured with a standard four-terminal method. Samples were cut into a thin bar with typical size of  $4\text{mm} \times 2\text{mm} \times 0.5\text{mm}$ . Gold wires were attached onto the samples' newly-abraded surface with silver paint. The size of the contact pads leads to a total uncertainty in the absolute values of resistivity of 10 %. The electrical resistance was measured using a steady current of 5 mA, after checking the linear  $I - V$  characteristic.

Temperature dependence of magnetization was measured on a Quantum Design Magnetic Property Measurement System (MPMS-5). For the measurement of the undoped compound, the applied field was 1000 Oe. For the measurement of the Th-doped superconducting samples, both the zero-field-cooling and field-cooling protocols were employed under the field of 10 Oe.

[1] Kamihara, Y. *et al.* Iron-based layered superconductor  $\text{La}[\text{O}_{1-x}\text{F}_x]\text{FeAs}$  ( $x=0.05-0.12$ ) with  $T_c=26$  K. *J. Am. Chem. Soc.* **130**, 3296-3297 (2008).  
 [2] Takahashi, H. *et al.* Superconductivity at 43 K in an iron-based layered compound  $\text{LaO}_{1-x}\text{F}_x\text{FeAs}$ . *Nature* **453**, 376-378 (2008).  
 [3] Chen, X. H. *et al.* Superconductivity at 43 K in samarium-arsenic oxides  $\text{SmFeAsO}_{1-x}\text{F}_x$ . *Nature* **354**, 761-762 (2008).

[4] Chen, G. F. *et al.* Superconductivity at 41 K and its competition with spin-density-wave instability in layered  $\text{CeO}_{1-x}\text{F}_x\text{FeAs}$ . *Phys. Rev. Lett.* (in press), arXiv:0803.3790v3 (2008).  
 [5] Ren, Z. A. *et al.* Superconductivity at 52 K in iron-based F-doped layered quaternary compound  $\text{Nd}[\text{O}_{1-x}\text{F}_x]\text{FeAs}$ . *Europhysics Lett.* **82**, 57002 (2008).  
 [6] Ren, Z. A. *et al.* Superconductivity at 52 K in iron-based F-doped layered quaternary compound  $\text{Pr}[\text{O}_{1-x}\text{F}_x]\text{FeAs}$ .

- arXiv:0803.4283 (2008).
- [7] Ren, Z. A. *et al.* Superconductivity at 55 K in iron-based F-doped layered quaternary compound  $\text{Sm}[\text{O}_{1-x}\text{F}_x]\text{FeAs}$ . arXiv:0804.2053 (2008).
- [8] Liu, R. H. *et al.* Phase diagram and quantum phase transition in newly discovered superconductors:  $\text{SmO}_{1-x}\text{F}_x\text{FeAs}$ . *Chin. Phys. Lett.* **25**, 2215-2216 (2008).
- [9] Ren, Z. A. *et al.* Novel superconductivity and phase diagram in the iron-based arsenic oxides  $\text{ReFeAsO}_{1-\delta}$  (Re = rare earth metal) without F-doping. arXiv:0804.2582 (2008).
- [10] Chen, G. F. *et al.* Element substitution effect in transition metal oxyphnictide  $\text{Re}(\text{O}_{1-x}\text{F}_x)\text{TAs}$  (Re=rare earth, T=transition metal). *Chin. Phys. Lett.* **25**, 2235-2238 (2008).
- [11] Cheng, P. *et al.* Superconductivity at 36 K in gadolinium-arsenide oxides  $\text{GdO}_{1-x}\text{F}_x\text{FeAs}$ . *Science in China G* **51**, 719-722 (2008).
- [12] Quebe, P., Terbuchte, L. J. & Jeitschko, W. Quaternary rare earth transition metal arsenide oxides  $\text{RTAsO}$  (T=Fe, Ru, Co) with  $\text{ZrCuSiAs}$  type structure. *J. Alloys and Compounds* **302**, 70-74 (2000).
- [13] Johnson, V. & Jeitschko, W. J.  $\text{ZrCuSiAs}$ : a "filled"  $\text{PbFCl}$  type. *Solid State Chem.* **11**, 161-166 (1974).
- [14] Shannon, R. D. Revised effective ionic radii and systematic studies of interatomic distances in halides and chalcogenides. *Acta Crystallogr. Sect. A* **32**, 751-767 (1976).
- [15] Cava, R. J. Oxide superconductors. *J. Am. Ceram. Soc.* **83**, 5-28 (2000).
- [16] Yang, J. *et al.* Superconductivity at 53.5 K in  $\text{GdFeAsO}_{1-\delta}$ . *Supercond. Sci. Technol.* **21**, 082001 (2008).
- [17] Tokura, Y., Takagi, H. & Uchida, S. A superconducting copper oxide compound with electrons as the charge carriers. *Nature* **337**, 345-347 (1989).
- [18] Dong, J. *et al.* Competing orders and spin-density-wave instability in  $\text{La}(\text{O}_{1-x}\text{F}_x)\text{FeAs}$ . arXiv:0803.3426v1 (2008).
- [19] Cruz, C. *et al.* Magnetic order versus superconductivity in the iron-based layered  $\text{La}(\text{O}_{1-x}\text{F}_x)\text{FeAs}$  systems. *Nature* **453**, xxx-xxx (2008), in press, doi:10.1038/nature07057.
- [20] McGuire, M. A. *et al.* Evidence for the spin density wave in  $\text{LaFeAsO}$ . arXiv:0804.0796v1 (2008).
- [21] Nomura, T. *et al.* Crystallographic phase transition and high- $T_c$  superconductivity in  $\text{LaOFeAs:F}$ . arXiv:0804.3569v1 (2008).
- [22] Ding, L. *et al.* Specific heat of iron-based high- $T_c$  superconductor  $\text{SmO}_{1-x}\text{F}_x\text{FeAs}$ . *Phys. Rev. B* **77**, 180510R (2008).

### Acknowledgments

The authors thank Fuchun Zhang, Ying Liu and Xi-anhui Chen for helpful discussions. This work is supported by the National Basic Research Program of China (No.2006CB601003 and 2007CB925001) and the PCSIRT of the Ministry of Education of China (IRT0754).